PROCEEDINGS OF SPIE

SPIEDigitalLibrary.org/conference-proceedings-of-spie

ELT METIS wavefront control strategy

Carlos Correia, Markus Feldt, Horst Steuer, Julia Shatokhina, Andreas Obereder, et al.

Carlos M. Correia, Markus Feldt, Horst Steuer, Julia Shatokhina, Andreas Obereder, Philip Neureuther, Martin Kulas, Hugo Coppejans, Gilles Orban de Xivry, Silvia Scheithauer, Thomas Bertram, "ELT METIS wavefront control strategy," Proc. SPIE 12185, Adaptive Optics Systems VIII, 1218512 (29 August 2022); doi: 10.1117/12.2630096

SPIE.

Event: SPIE Astronomical Telescopes + Instrumentation, 2022, Montréal, Québec, Canada

ELT METIS wavefront control strategy

Carlos M. Correia[a], Markus Feldt[b], Horst Steuer[b], Julia Shatokhina[c], Andreas Obereder[c], Philip Neureuther[d], Martin Kulas[b], Hugo Coppejans[b], Gilles Orban de Xivry[e], Silvia Scheithauer[b], and Thomas Bertram[b]

[a]Space ODT – Optical Deblurring Technologies, Porto, Portugal
[b]Max-Planck-Institut für Astronomie, Königstuhl 17, 69117 Heidelberg, Germany
[c]Johann Radon Institute for Computational and Applied Mathematics, Linz, Austria
[d]Univ. Stuttgart, Germany
[d]Univ. Liège, Belgium

ABSTRACT

METIS is the European Extremely Large Telescope (ELT) 1st-generation Mid-Infrared ELT Imager and Spectrograph. It will offer spectroscopic, imaging and coronagraphic capabilities from 3 up to 13 microns with Adaptive-Optics correction.

With its Final Design Review due late 2022 we report on the wavefront control strategy devised to meet the METIS science and technological requirements. Such strategy addresses challenging aspects as i) the appearance of differential petal piston modes in the presence of secondary mirror support struts caused either by numerical processing or the actual, physical low-wind effect, ii) the numerical pupil derotation and mis- reg compensation, iii) the adaptation to transient disturbance signals such as telescope-to-instrument handover control and iv) the compliance with constrained modal control of the pre-focal beam corrector mirrors (M4/M5).

The overall METIS wavefront control strategy consists in a split approach cemented in a sequence of steps: 1) Tikhonov-regularised spatial wavefront estimation/reconstruction on a zonal Cartesian coordinate system tied to the pyramid (P-WFS) sampling pixel grid, 2) the regularised projection onto a global modal control space including correction of mis-registrations and rotation between the P-WFS coordinate grid and the ELTs M4/M5, and 3) the time-filtering through the application of proportional-integral control before converting to actuator commands readied for the ELTs collaborative TT off-loading scheme whilst avoiding hitting the mirrors constraints in amplitude, speed and force.

We present physical-optics simulation results of the whole AO system obtained with prototyped instances of the real-time and soft-real-time computers including sensitivity analysis with respect to observational, atmospheric, non-atmospheric (telescope-intrinsic such as wind-induced low-order modes comprising tip-tilt) and instrument-specific conditions and disturbances.

An error budget is put together that meets the METIS science requirements in terms of wavefront error with reassuring margins thus endorsing the strategy devised.

Keywords: Adaptive Optics, Wavefront Reconstruction, Dynamic Control

1. INTRODUCTION

The Mid-infrared ELT Imager and Spectrograph (METIS) is one of three first-light instruments on the European Extremely Large Telescope (ELT).

METIS covers the mid-infrared/thermal spectral range between 3 13 microns. Diffraction limited imaging, coronagraphy, medium resolution (R 102 - 103) slit spectroscopy over the full spectral range (starting at 3 m) and high resolution (R 105) integral field spectroscopy in the lower spectral range (2.9 5.3 m) make METIS a versatile instrument. The compact imaging field of view of 10 x 10 together with a much larger isoplanatic

Further author information: (Send correspondence to Carlos Correia)
E-mail: cmcorreia@spaceodt.net

Adaptive Optics Systems VIII, edited by Laura Schreiber, Dirk Schmidt, Elise Vernet,
Proc. of SPIE Vol. 12185, 1218512 · © 2022 SPIE
0277-786X · doi: 10.1117/12.2630096

angle of about 20 for the shortest science wavelength and median atmospheric conditions, clearly indicate the need for a single conjugate adaptive optics (SCAO) system to achieve diffraction limited performance.

A PDR analysis was conducted with the main results accessible in.[1] For the FDR version we revisit the assumptions and update the overall METIS SCAO control strategy.

This document covers the general aspects related to the standard disturbance-rejection control problem at the core of the SCAO, the mathematical bases used to represent discretised signals and the practical implementation we retained for our baseline solution in terms of

1. Spatial wave-front reconstruction
2. Dynamic time-filtering, including anti-windup and saturation avoidance strategies Auxiliary control loops and loop co-processing optimisation tasks are also discussed.

2. METIS WAVE-FRONT CONTROL STRATEGY

Figure 1 depicts schematically the METIS SCAO system and its main submodules. The SCAO Real-Time Computer (RTC) is subdivided into hard (HRTC) and soft (SRTC) each with its specific processing functions.

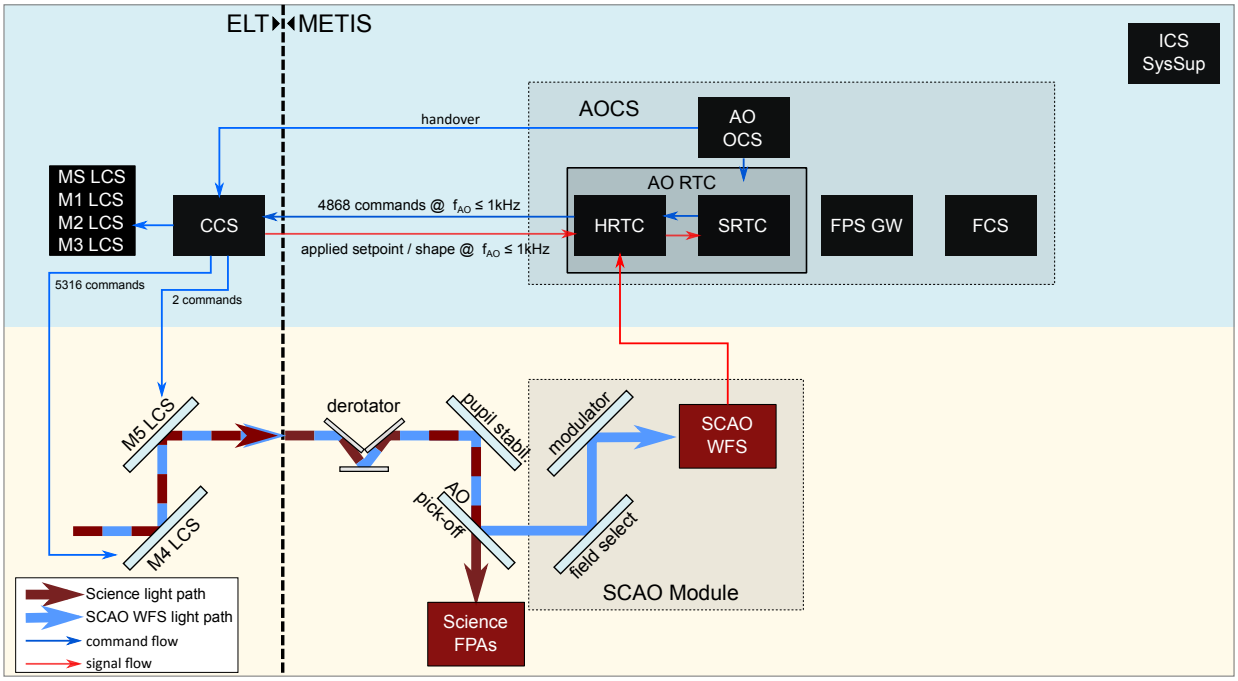

Figure 1. METIS SCAO overview: The components inside the grey boxes are part of METIS SCAO. Those devices inside the dotted box labelled with ELT are part of the ELT infrastructure. Red arrows indicate measurement signal flow, blue arrows command flow. Red boxes represent sensors, black boxes represent control services. The Hard Real-Time Core (HRTC) within SCAO RTC is responsible for the core wave-front control loop. Data products that rely on SCAO telemetry are computed in the Soft Real-time Cluster (SRTC). The INS AOC comprises also the AO FCS to accomplish secondary control tasks, such as modulation and field selection.

The interfacing between the instrument (INS) and the telescopes central control system (CCS) is made via a vector with 4868 coefficients with the first four entries representing residual and *requested* TT respectively. The remainder are the HO requests expressed on a proper control basis. The matrix of *modes-to-commands* (**M2C**) whose columns represent linear combinations of M4 actuator commands generating the control modes is passed on to the CCS such that the requests originally expressed in the control basis can be mapped onto M4 setpoints, once past the saturation handling and safety checks. The exact definition of the latter and the policies to be

followed are still under refinement by ESO. In our baseline we devised several saturation avoidance policies that rely on penalising both spatially and temporally the actuator command requests sent to M4. On top of this, we do leave the option open for a governor constrained controller to provide best performance under real conditions should it be required. It has been extensively studied in.[2]

2.1 METIS SCAO performance requirements

The METIS baseline control strategy was put together with the following goals in mind:

1. Deliver at least 93% Strehl (goal: 95%) at 10 mum, and at least 60% (goal: 80%) Strehl at 3.7 mum
2. Keep the dierential segment piston error below 28 nm rms
3. Support both field- and pupil-tracking modes with no derotator in the WFS path

2.2 Baseline control strategy & additional options foreseen

These requirements then led to some design choices

1. Controlling the maximum number of M4 degrees-of-freedom without generating unwanted spurious signals (e.g. differential-piston modes) with a 90x90 Pyramid WFS (PWFS) in K-band
2. Performing numerical derotation when in field-trackling mode and streamlined on-the-fly reconstructor updates, including mis-reg management
3. Using a set of aperture-spanning modes as a control basis ranked jointly by increasing spatial frequency and force on M4

Based on these we have converged on a split spatial reconstruction / temporal filtering which is schematically represented in Fig. 2.

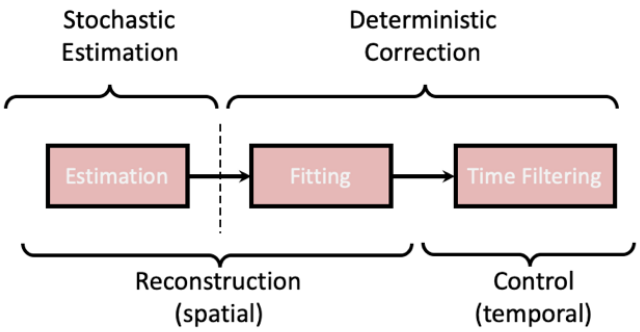

Figure 2. Separation between stochastic estimation and deterministic correction, spatial reconstruction and temporal, dynamic control. This over-simplification shows the interplay of the different, spatial and temporal, stochastic and deterministic operations. The estimation and fitting, whereas both spatial filtering operations, are two distinct steps. This is a feature we retained since the pupil and DM actuator mesh optically rotate in front of the P-WFS. Decoupling the reconstruction from the fitting is an aspect of significance that is considered in our developments for it allows for a streamlined implementation and AO system adaptation to changing conditions.

In our solution, we first solve for the wave-front *spatial reconstruction* neglecting any temporal evolution and postulate an a-priori PI controller structure for the time-filtering (a.k.a. regulators or controllers), both for TT and ho modes.

The reconstruction step is further sub-divided into two steps: i) the stochastic wavefront estimation from PWFS data and ii) the deterministic fitting/projection onto the desired control space.

The strategy outlined here tackles both steady-state and transient behaviour.

In a nutshell the METIS wavefront control strategy can be summarised as follows:

- Pixel processing and computation of so-called *slopes-maps* normalised by the integrated flux collected on the four re-imaged pupils
- Wavefront control
  - Spatial reconstruction
    - Tikhonov-regularised stochastic estimation expressed on the space formed by the influence functions of a Cartesian-mesh virtual DM layout
    - a fitting/projection step onto control modes
      - Force-aware Karhunen-Loeve modes
      - Derotation and mis-reg compensation via linear-algebra operations
  - Time-filtering
    - PI control for TT and HO modes
    - Anti-windup through error deflation using the CCS feedback (a.k.a. "echo")
  - Saturation avoidance
    - Modal loop gain adjustment
    - Regularisation strength adjustment on the fitting step between reconstruction and M4 space

Furthermore, we envision the use of leaky controllers which proved useful in the deployment of many AO systems on-sky potentially supplemented with

- vibration rejection mostly to mitigate wind-induced TT
- constrained control using a governor which applies modifications to the control requests to avoid M4 constraints and the subsequent performance losses[2]

Predictive control (either in the form of the optimal Minimum-Variance solution or otherwise) is not planned to be implemented as of now.

3. MAIN CONTROL LOOP

In our baseline we chose to use two distinct spaces

- Reconstruction: the set of continuous influence functions of a Cartesian-mesh virtual DM layout with 20% cross-coupling
- M4 control: the set of principal components of the atmospheric spectrum projected onto the M4 space via a regularised decomposition that conserves *globally* the mode ranking by increasing spatial frequency* whilst penalising the forces on M4.[3] These modes are referred to as *Force-aware Karhunen-Loeve* modes in the remainder.

*This is not an exact statement since the decomposition by construction generates modes that do not correspond to individual spatial frequencies, yet are commonly dominated by a small enough subset to allow us the use of this somewhat loose terminology.

3.1 Spatial Reconstruction

3.1.1 Wavefront estimation from PWFS signals

To cope with closed-loop operation, in our implementation we will deviate from the nominal minimum-mean-square-error (MMSE) solution. We use instead a related Tikhonov-regularised spatial wavefront estimator defined on the set of influence functions (Gaussian-like with 20% coupling) laid out on a Cartesian 2-D mesh on each corner of the PWFS sub-apertures (therefore called VDM)

$$\mathbf{R} = \left(\mathbf{W}_{\mathsf{VDM}}^{\mathsf{T}}\mathbf{W}_{\mathsf{VDM}} + \omega_{rec}\nabla^4\right)^{-1}\mathbf{W}_{\mathsf{VDM}}^{\mathsf{T}} \tag{1}$$

where ∇^4 is a sparse discrete squared Laplacian (also called bi-harmonic) matrix representation with ω_{rec} a weighting scalar and $\mathbf{W}_{\mathsf{VDM}}$ is a concatenation of synthetic P-WFS responses to each individual VDM actuator through a model of the M1 pupil (+ spiders) in the absence of AO residuals yet using a modulated sensor.

The reconstruction is followed by a fitting/projection step onto the modal control space of our choice as shown next.

3.1.2 Fitting and change of control space

The fitting step is the deterministic, Tikhonov-regularised projection from VDM space onto the control space defined on the set of force-aware Karhunen-Loève modes (KL).[3]

In the absence of pupil rotation, we have nominally:

$$\bar{\mathbf{u}}_k^{\mathsf{M4}} = \mathbf{M2C}_0\mathbf{m}_k \tag{2}$$

where $\mathbf{M2C}_0$ is the *modes-to-commands* matrix computed for a nominal rotation angle – that we assume without loss of generality to be "0" (zero). Each of its columns provides the set of linearly combined M4 commands which produce each and every predefined KL mode.

The modal coefficient set is computed at time step k from

$$\mathbf{m}_k = \mathbf{M2C}_0^{\dagger}\left(\mathbf{N}_{\mathsf{M4}}^{\mathsf{T}}\mathbf{N}_{\mathsf{M4}} + \omega_{fit}\nabla^4\right)^{-1}\mathbf{N}_{\mathsf{M4}}^{\mathsf{T}}\mathbf{N}_{\mathsf{VDM}}\mathbf{u}_k^{\mathsf{VDM}} \tag{3}$$

where we adopt as smoothing function the same squared Laplacian matrix yet scaled differently and defined on the M4 actuator coordinates (not the regular VDM coordinates). This smoothing function provides a stable projection between the wave-front reconstruction space (the VDM) and the M4 command space. Furthermore once optimised, it gives us the ability to control all the modes and therefore optimise the performance.

The matrix $\mathbf{M2C}_0$ is computed off-line (using the algorithm from[3] and communicated to the CCS which computes the set of M4 actuator positions *requested* by the instrument before the saturation handling algorithm is activated.

3.1.3 Numerical derotation and mis-reg management

METIS shall support numerical derotation for field-tracking mode. In this case, the field is optically derotated on the science channels yet the pupil (and the M4 mesh) rotate on the PWFS.

Having decoupled the estimation from the fitting/projection now allows us a straighforward implementation of numerical derotation. The latter intervenes at both the reconstruction and fitting steps.

Our strategy consists in pre-computing and storing a set of interaction matrices that span a 60-degree rotation (periodic pattern). This assumes the pupil is kept in place to better than 1/10th of a pixel and that any dierential lateral motion between M4 and the pupil is compensated via the mis-registration idenfication and control. The use of a unique meta interaction matrix is not excluded at this point. The mis-reg is solely associated with the fitting step based on a parameter set provided by processing system telemetry and geometric models for the rotation and other common mis-reg errors such as shifts and (differential) magnification.

The modes-to-commands **M2C** matrix remains constant over time. It is published by the instrument and subscribed to by the CCS. However, since M4 rotates with respect to a reference coordinate system attached to the wave-front sensor (and consequently the VDM), the modal coefficients are computed as follows

$$\bar{\mathbf{u}}_0^{\mathsf{M4}} = \mathbf{M2C}_0 \mathbf{m}_\theta \tag{4}$$

$$\mathbf{m}_\theta = \mathbf{M2C}_0^\dagger \mathbf{N}_{\mathsf{M4}}^\dagger(-\theta)\mathbf{N}_{\mathsf{VDM}}\mathbf{u}_\theta^{\mathsf{VDM}} \tag{5}$$

$$\mathbf{u}_\theta^{\mathsf{VDM}} = \mathbf{R}_\theta \mathbf{s} \tag{6}$$

where we used abbreviated notation for the regularised pseudo-inverse of $\mathbf{N}_{\mathsf{M4}}$.

It is now clear that as much as with rotation, other mis-reg parameters will be dealt with by generalising Eq. (5) for a set of parameters $\mathcal{P} = \{\Delta_x, \Delta_y, \theta, \cdots\}$

$$\mathbf{m}_\mathcal{P} = \mathbf{M2C}_0^\dagger \mathbf{N}_{\mathsf{M4}}^\dagger(-\mathcal{P})\mathbf{N}_{\mathsf{VDM}}\mathbf{u}_\mathcal{P}^{\mathsf{VDM}} \tag{7}$$

In Eq. (7) (similarly to Eq. (5)) we use the notation $-\mathcal{P}$ to indicate the instantiation of projection matrices with reversed sign mis-reg parameters.

3.1.4 Computation of M2C

The $\mathbf{M2C} \in \Re^{4866\times 4866}$ matrix is a modified version of the original $\overline{\mathbf{M2C}} \in \Re^{5352\times nCtrModes}$ natively generated when computing the Karhunen-Loeve[†] modes which span the whole M4 control space.[3] **M2C** computed as follows

$$\{\mathbf{M2C}\} = \mathbf{X} \cdot \overline{\mathbf{M2C}} \tag{8}$$

where $\mathbf{X} \in \Re^{4866\times 5352}$ is a zero-one-valued matrix that truncates actuator requests outside of available actuator range.It is concatenated with a zero-valued matrix to obtain correct matrix sizes should we use less control modes than available M4 degrees-of-freedom.

3.1.5 Modulation

Extensive simulations showed that a circular modulation with $4\lambda/D$ radius provides near-optimal performance for all observing conditions. We do expect the system to be able to run with lower modulation, down to $\sim 2\lambda/D$.

On the other hand, water vapour seeing correction made via reference PWFS signals does benefit from a larger modulation (larger dynamic range). Yet this implies pre-computing a larger set of interaction matrices which we otherwise avoid by operating the system at a single modulation radius of $4\lambda/D$.

3.1.6 Optical gains

Optical gain(s) refer to the PWFS sensitivity when working off its calibration setpoint.

In the case of METIS, the sensitivity loss is estimated to be rather small[4] and we plan to compensate for it by optimising the closed loop modal gains only.

3.1.7 Saturation Avoidance

Saturation avoidance (dual of the saturation handling done by the CCS) refers to the means employed by METIS to avoid hitting the M4 constraints.

A first level of saturation avoidance is provided by the use of a *force-aware* M4 control basis (cf. §**??**) which grants a balanced trade-off between fitting error and force in its definition.

On top of this, other options are available to us. We plan to use the following policies either separatly or jointly

[†]Although this needs not strictly be the case, the basis is generated such that orthogonality is imposed with respect to the M1 pupil yet all the actuators – which span an area larger than M1 – are used in its generation.

(i) Mode truncation by setting to zero (or very low values) the corresponding control loop gains (acts on the temporal filtering domain) or removing the modes from the projection matrices (acts on the spatial reconstruction domain)

(ii) Linear penalties on either the Reconstruction (ω_{rec} in Eq. 1) or Fitting/Projection step (ω_{fit} in Eq. 3) or both (acts on the spatial reconstruction)

A strategy like in (i) (done at LBT for instance) shall relieve us from hitting M4 control constraints (see[?] for the analysis). Option (ii) provides extra regulation shall it be needed during steady-state runtime operations. Both can be implemented at the expense of system performance.

Section 3.2.5 provides a constrained-control option that shall be considered only if the other options fail to provide meaningful performance results. Adding it to our real-time pipeline represents a considerable increase in computational load.

3.2 Dynamic control (aka Time-filtering) under the sequential handover scenario

We place ourselves under a sequential handover scenario whereby the AO system is driven by the METIS WFS only (opposed to using jointly the telescope guide-probes under a cascaded scenario). The design of a stabilising controller C4 for both TT and HO modes falls entirely under METIS as we shall show next. We provide a likely operational scenario with integral+proportional action control, some leakage factor and anti-windup through error deflation, of which an illustration is shown in Fig. 3.

Under the sequential scenario, the high-order modes are nominally fed to M4 unfiltered unless saturation handling is activated and eventually any other CCS AO tasks should the METIS requests oend the m4 control constraints.

We consider the general case where the temporal filter is applied through an Infinite Impulse Response (IIR) filter to an error signal $\mathbf{e}_k^-$ in the form

$$\mathbf{m}_k = \sum_{j=0}^{P_{IIF}} b_j \mathbf{e}_{k-j}^- - \sum_{i=1}^{Q_{IIF}} a_i \mathbf{m}_{k-i} \tag{9}$$

where

- $\mathbf{e}_{k-j}^-$ is the error signal expressed in the control modal basis. The upperscript $^-$ expresses the error before the windup correction is applied (see §3.2.3)
- P_{IIF} and Q_{IIF} the orders of the IIR numerator and denominator

In practice we will replace $\mathbf{e}_{k-j}^-$ in Eq. (9) by $\mathbf{e}_{k-j}$ in Eq. (12) to wind down the controller should any saturation or mode truncation be applied by the CCS upon METIS control requests.

3.2.1 Integral and Proportional control

METIS baseline is to use order 1 IIR filters in Eq. (9). A leaky Proportional-Integral controller implements the recursion

$$\mathbf{m}_k = \gamma \mathbf{m}_{k-1} + (g_I - g_P)\mathbf{e}_k - g_P \mathbf{e}_{k-1} \tag{10}$$

whose Z-transform is

$$h_{\mathsf{C4}}(z) = \left(\frac{g_I}{1 - z^{-1}} + g_P \right) = \frac{z(g_I + g_P) - g_P}{z - 1} \tag{11}$$

3.2.2 Frame-rate

METIS will adapt its pwfs integration time and therefore the control loop frame-rate as a function of NGS brightness. This is a normal procedure to increase the limiting magnitude of an instrument see for instance[5] for related examples.

3.2.3 Anti-windup strategy

The potential nefarious effects of integral action windup are well known. Figure 3 illustrates the effect in response to a step input when no anti-windup is applied or when the error is deflated using the difference between the requested and applied commmands.

METIS will receive an echo signal to compute an error signal $\boldsymbol{\epsilon}$ that shall be used to wind down its control loops. The solution we advocate is to deflate the error signal in Eq. (9) by modifying the error

$$\mathbf{e}_k = \mathbf{e}_k^- - \mu_{\text{aw}}\boldsymbol{\epsilon}_k \tag{12}$$

to include the difference between the instrument-requested and CCS-applied commands expressed in an agreed-upon modal basis:

$$\boldsymbol{\epsilon}_k = \mathbf{m}_{k-1} - \widehat{\mathbf{m}}_{k-1} \tag{13}$$

where

- $\mathbf{m}_{k-1}$ are the *requests* expressed in the METIS modal basis requested from M4. We can call them requests to account for the subtle, yet real, different between what is requested and actually applied.
- $\widehat{\mathbf{m}}_{k-1}$ is the echo signal sent back by the CCS corresponding to the actual applied commands, expressed in the instrument control basis. These may differ from the requests on account of exceeding operational limits as per;[?]
- μ_{aw} is a scalar weight whose default value is 1

In practice we may need to adjust the weighting factor before $\boldsymbol{\epsilon}_k$ for performance purposes. In the absence of saturation management and DM dynamics this term is null.

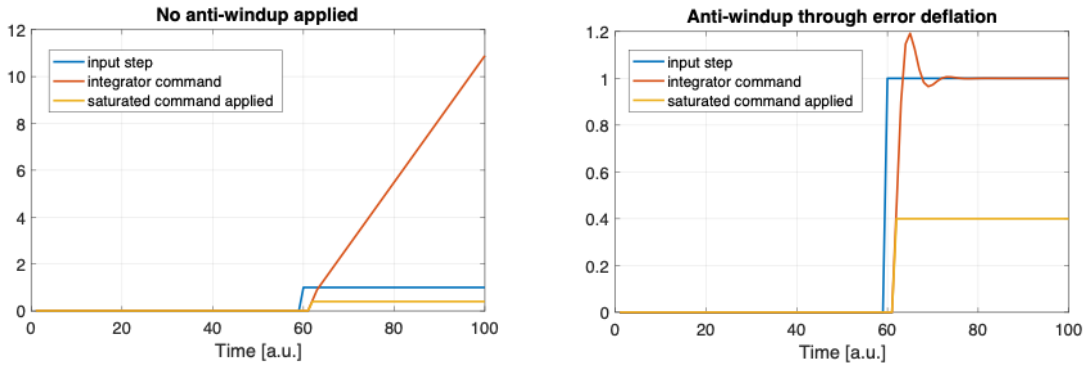

Figure 3. Anti-windup illustration when error deflation is taken into account.

3.2.4 Vibration feed-forward control

An optional feed-forward vibration controller is considered. It is an optional add-on to the SCAO feedback controller and improving the rejection of vibration-induced wave-front disturbances. The basic idea underlying this feed- forward concept is that the wave-front disturbance caused by vibrations essentially consist of a few spatial modes and temporal frequencies. For example, tip or tilt are dominant in wind-induced disturbances at the ELT and feature distinct peaks in their temporal spectra. The feed-forward concept is depicted in Fig. 4. Within an EP filter, an extended Kalman filter estimates the states and parameters of the associated oscillators and a model-based prediction is conducted to compensate for time delays (cf. Fig. 4). The vibration feed-forward as well as the SCAO feedback controller shall be evaluated in parallel on the METIS RTC and the feed-forward

must be designed carefully to ensure a stable and beneficial collaboration with the feedback controller. If the open-loop disturbance dwf is dominated by the vibration- induced disturbance dvib for some characteristic modes, the METIS SCAO performance w. r. t. to these modes significantly improves through the presented feed-forward. In principal, the feed-forward can accommodate an arbitrary number of characteristic modes and frequencies, which are not restricted to the bandwidth of the SCAO control loop. Hence, the feed-forward is an interesting optional add-on for the baseline SCAO controller.

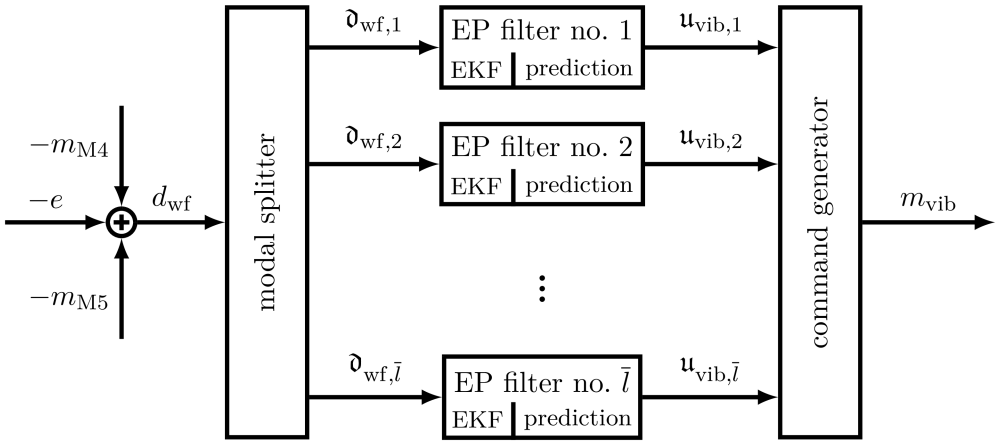

Figure 4. Block diagram of the feed-forward concept based on the characteristic modes and frequencies of vibrations.

3.2.5 Saturation Avoidance via constained dynamic control

In the previous sections we discussed several strategies to consider M4 constraints in the SCAO controller and prevent integral action windup or similar effects. For the (unlikely) case that the SCAO system cannot be operated satisfactorily using any of these strategies, we developed and studied the so-called spatio-temporal error governor (STEG).

The STEG is an add-on for the baseline SCAO feedback controller and modifies the control error before it is fed into the SCAO controller. Within the error modification, the STEG considers the spatio-temporal and segmented characteristics of M4 and aims for the best SCAO performance while adhering to all M4 constraints. Additionally, the STEG features the following beneficial properties, among others:

- Add-on for the SCAO feedback controller,
- No permanent trade-off between performance and constraint compliance,
- Availability of three algorithms implementing the STEG and featuring different characteristics,
- Application of numerically cheap approximating models.

Moreover, we successfully verified the functionality of the STEG and its algorithms in a conceptual study.[2]

Please note that the implementation and computational effort for the STEG is much higher compared to any strategy handling constraints, which has been discussed previously. Therefore, the STEG is not the baseline strategy to consider M4 constraints in the SCAO controller, but is the last resort if no alternative strategy can be successfully operated. Further information and discussions on the STEG and its algorithms are presented in.[2]

3.3 Transient handling

3.3.1 Telescope handover

In the following we provide the general approach which involves the following main stages:

1. The Pupil-Position Control (PPC) loop is engaged with the pupil stabilised on the PWFS detector
2. Hand-shaking phase during which CCS TT commands are shared with the INS to ensure a bumpless transition
3. Handover control of a set of low-order modes including tip-tilt
4. Trigger the mis-registration algorithm
5. Control a higher number of modes
6. Repeat 4. and 5. until the pre-defined number of control modes is achieved

During this handover phase, we may need to update the control matrix based on the mis-reg parameters estimated during loop closure. This may result from any differential motion and/or optical warping between the pupil and M4 which will then be estimated via our chosen mis-reg algorithm. Otherwise the pupil stabilised in lateral motion by the PPC loop will grant only a sub-pixel residual. The observation model from which the rotation is inferred will then be used to numerically derotate the pupil via our DM projection step.

We note that any unknown lateral motion and/or magnification will have no implication on our Interaction Matrix (IM) calibration strategy (§**??**). The latter depends on the diffraction pattern generated by the M1 pupil whose transverse translations are stabilised with the PPC loop. Any mis-registrations will then be dealt with independently at the projection step.

3.3.2 ROUS

The baseline strategy consists in considering the Recurrent Optimisation of (M4) Units Stroke (ROUS) transient in much the same way we consider the bootsrapping transient after telescope handover.

Scheduling the ROUS METIS will schedule observations around rous events such that they are not at all impaired by such events. In order to enforce it metis will influence the time of execution to avoid negative impact on on-going observations.

Control loop adaptation During the rous, metis control loops will remain closed. Although our simulations show that the loop remains stable across the event with all modes controlled, in practice the rous will be crossed with a fewer number of actively controlled modes or a combination of strategies similar to the handover transient. In the likely event that the pupil and the mis-registration parameters change on account of the optical offoading, we will first stabilise the pupil to its nominal position, then deploy the mis-registration identification algorithm with the loop closed on a small subset of modes.

The transient is around 2-3s during which we expect a tilt excursion of $< 10\,mas$. Once this transient is over, pupil stabilisation and mis-registration management (if needed) are carried out. Past this period, nominal operations can resume.

4. AUXILIARY CONTROL LOOPS

The term auxiliary control loops refer to supporting loops that stabilise or adjust working setpoints needed for optimal performance. Due to the nature of the auxiliary control loops which involve system telemetry processing and/or control actions on actual hardware, they will be detailed separately below. Software optimisation tasks are covered in the next section.

1. **Pupil Position Control Loop** the PWFS pupils are stabilised using matched filters in a similar implentation to that of TMT.[6] In our case the template images fully rely on the jagged inner and outer edges of the primary pupil when spiders are removed.
2. **Differential Tip-Tilt Control Loop** diffential TT provided by QACITS[7] is compensated for using the modulation mirror, therefore leaving intact the WFS dynamic range which would have been otherwise reduced if we were to compensate dierential TT via slope offsets.
3. **Differential High-Order Control Loop** the differential high-order control loop compensates for NCPA and water-vapour seeing via PWFS slope offsets.

5. LOOP CO-PROCESSING TASKS

The METIS wavefront control strategy is supported by a number of *Loop Co-Processing* monitoring and optimisation tasks. These allow operating the system within requirements and allocated tolerances. In addition to the **Auxiliary Control Loops** (covered in §4) tasks under the following categories (see Table 1) will be executed in parallel to the control loops:

1. **System parameter estimation** – encompassing the tasks where geometric and optical parameters are estimated from telemetry and metrology accessible in the system
2. **Control loop parameter optimisation** – covering the tasks pertaining to the optimisation of control matrices, loop gains etc
3. **Statistics** & **Diagnostics** – where performance metrics are made available from the AO telemetry, science detectors and other internal metrology

Table 1. Loop co-processing monitoring and optimisation tasks.

System parameter estimation	Control loop parameter optimisation	Offsets, Statistics and Diagnostics
Pupil-position monitoring (lateral motion and clocking)	Regulator parameter optimisation	PSF Strehl-ratio, FWHM
Mis-reg identification	Control matrix optimisation	Contrast
Interaction matrix calibration		Pupil Fragmentation
Valid sub-apertures map		System performance estimates PSDs (temporal, spatial)
Valid actuators map		Telemetry statistics
		Saturation statistics

6. METIS ERROR BREAKDOWN

We can now anchor the error budget on the results presented in the preceding sections. Table 2 summarises the error budget by combining three main categories:

1. AO errors (evaluated with the analytic, synthetic and E2E tools)
2. Telescope errors (E2E tool only)
3. Instrument-specific errors (E2E tool only)

Table 2 shows the integrated METIS error budget. With all errors considered and with a 20% contingency the METIS SCAO is set to deliver on its promises and exceed the requirements listed in Sect. 2.1 (required and goal Strehl-ratio).

Table 2. Overall METIS error breakdown under a Cbasic configuration, median seeing conditions at 30deg zenith. The entries for apodisation and sensitivity loss originate from PDR estimates. Non-uniform reflectivity is an allocation that needs further consolidation.

Model:	Analytic	Synthetic (OOMAO)	E2E (COMPASS)	Synthetic (OOMAO)	E2E (COMPASS)	
Error Sources		L-band (3.7um)		N-band (10um)		**Units**
AO loop WFE budget						
Fitting error (M4 pitch = 0.5m)	100.6	107.9		107.9		nm
Aliasing error (PWFS pixel = 40/90 = 0.44m)	28.8	17.1		17.1		nm
Servo-lag error	30.0	17.5		17.5		nm
Photon + read noise	0.0	1.9		1.9		nm
Chromatism (30º zenith)		8.9		29.2		nm
Reconstuction error (from E2E)		38.0		38.0		nm
Segment piston error (from E2E)		17.0		17.0		nm
total AO residual wave-front error	108.8	118.6	122.9	121.8	122.9	nm
SR @ science wavelength		**96.0%**	**95.7%**	**99.4%**	**99.4%**	%
Telescope error budget						
Dynamic						
Wind-induced TT (1.4 mas rms)			68		68	nm
Wind-induced LO modes			18		18	nm
Wind-load on M1			15		15	nm
ROUS (transient event)			0		0	nm
Static						nm
M1 static (lin sum of 10 terms)			15		15	nm
M1 missing segments			27		27	nm
M1 reflectivity errors (2% non-uniformity)						
Instrument specific					0	nm
residual dispersion			18.4		18.4	nm
*apodised pupil (estimate from PDR)			45.3		45.3	nm
misregistration			50		50	nm
Calibration						nm
Residual NCPA			16.5		16.5	nm
PWFS optical defects (40 nm rms/axis/0.1 pixels)			56.6		56.6	nm
Median L0 = 100m instead of 25m			38		38	nm
Total non-AO residual WFE			126.2		126.2	nm
Total overall			**173.2**		**175.4**	**nm**
Total + Contingency (20%)			176.6		178.9	nm
Maréchal SR @ science wavelength			**91.4%**		**98.7%**	%

7. SAMPLE NUMERICAL RESULTS

In the following we show the result of a 60s long simulation when M4 is rotated 15^o with respect to the PWFS.

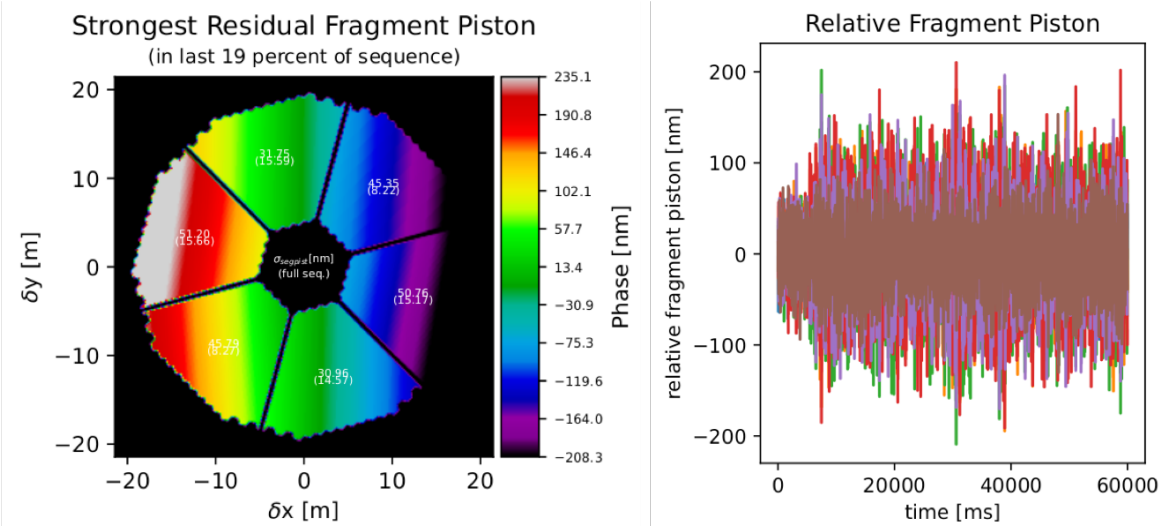

Figure 5. AOSAT output differential-piston on each of the M1 segments. Left: time-integrated values. Right: time-series.

The derotation is dealt with at the projection step by manipulating the linear-algebra projection of VDM influence-functions on the eigenmodes generated by a rotated M4. To complete the experiment, the **M2C** matrix used to convert modal coeffcients to actuator commands was the one computed for the nominal system (no rotation) as will happen in practice.

Figure 5 shows the output of a simulation for a 15^o rotation angle. The behaviour throughout time is almost indistinguishable from the nominal case, leading to very similar results indeed.

As a cross-check, the residual wavefront is also very smooth as shown in Fig. 6-left with the long-exposure PSF in Fig. 6-right a rotated version of the nominal one (we do not simulate a field rotator).

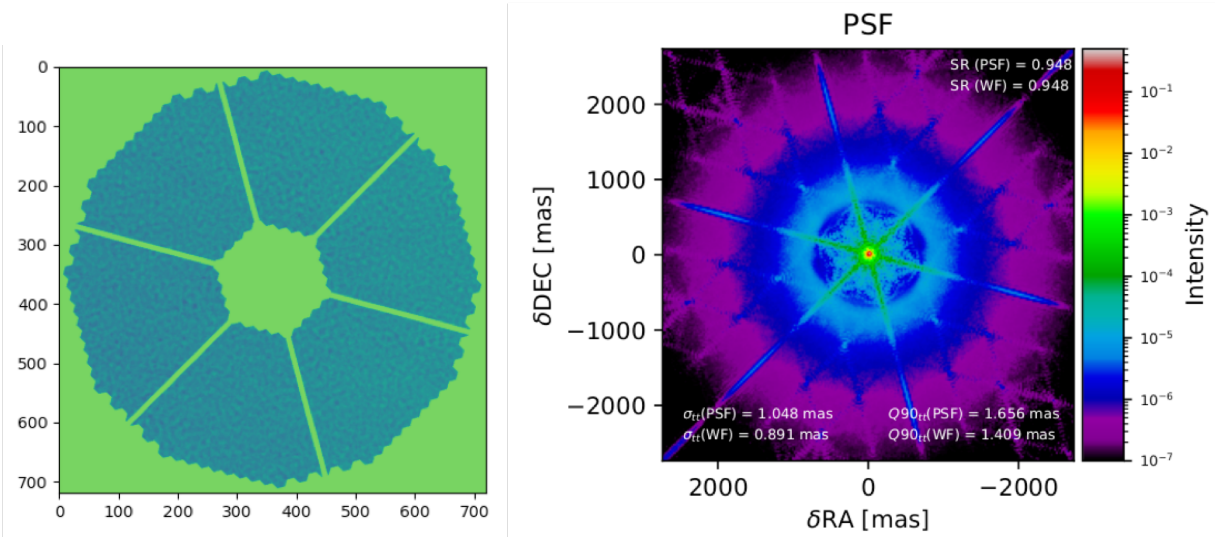

Figure 6. Wavefront residual at the end of the simulation. The residual is evenly distributed across the aperture and we note the absence of any edge effects.

8. SUMMARY

The wavefront control strategy outlined here meets the performance requirements set forth for the METIS SCAO module, both in terms of delivered Strehl-ratio – where both the requirement and goals are exceeded – but specially keeps the unwanted differential-piston below the 28 nm rms requirement for median seeing conditions at 30^o zenith. Moreover this nefarious mode is never excited to unacceptable levels nor the system gets stuck at multiples of λ_{WFS} for any of the seeing quartiles and magnitudes $\in \{4-12\}$ tested. Overall once the regularisation strengths for the reconstruction and projection steps were fixed, we could use them on all observing conditions METIS is likely to operate.

REFERENCES

[1] Hippler, S., Feldt, M., Bertram, T., Brandner, W., Cantalloube, F., Carlomagno, B., Absil, O., Obereder, A., Shatokhina, I., and Stuik, R., "Single conjugate adaptive optics for the ELT instrument METIS," *Experimental Astronomy* (Nov. 2018).

[2] Neureuther, P. L., Bertram, T., and Sawodny, O., "Control oriented strategy to consider constraints of the deformable mirror M4 for the Mid-infrared ELT Imager and Spectrograph," *Journal of Astronomical Telescopes, Instruments, and Systems* **8**, 1–24 (June 2022).

[3] Verinaud, C., "Tutorial for Force-optimized Modal Basis computation," tech. rep., ESO (Nov. 2020).

[4] Heritier, C. T., "Pseudo-Synthetic Interaction matrices for ELT Instrument SCAO Systems Analysis Report: Mis-registration Online Tracking," tech. rep., ESO (May 2022).

[5] Correia, C. M., Fauvarque, O., Bond, C. Z., Chambouleyron, V., Sauvage, J.-F., and Fusco, T., "Performance limits of adaptive-optics/high-contrast imagers with pyramid wavefront sensors," *Monthly Notices of the Royal Astronomical Society* **495**, 4380–4391 (06 2020).

[6] Véran, J.-P., Herriot, G., Andersen, D., and Wang, L., "Solving the NFIRAOS calibration puzzle," in [*Adaptive Optics Systems V*], Marchetti, E., Close, L. M., and Véran, J.-P., eds., *Society of Photo-Optical Instrumentation Engineers (SPIE) Conference Series* **9909**, 99090L (July 2016).

[7] Huby, E., Baudoz, P., Mawet, D., and Absil, O., "Post-coronagraphic tip-tilt sensing for vortex phase masks: The QACITS technique," *Astronomy and Astrophysics* **584**, A74 (Dec. 2015).